
Effects of Forced and Free Convections on Structural Temperatures of Space Shuttle Orbiter During Reentry Flight

William L. Ko, Robert D. Quinn, and Leslie Gong
Ames Research Center, Dryden Flight Research Facility, Edwards, California

1986
Revised June 1987



National Aeronautics and
Space Administration
Ames Research Center
Dryden Flight Research Facility
Edwards, California 93523-5000

EFFECTS OF FORCED AND FREE CONVECTIONS ON STRUCTURAL TEMPERATURES OF SPACE SHUTTLE ORBITER DURING REENTRY FLIGHT

William L. Ko,* Robert D. Quinn,** and Leslie Gong**
NASA Ames Research Center
Dryden Flight Research Facility
Edwards, California

Abstract

Structural performance and resizing (SPAR) finite-element thermal analysis computer program was used in the heat transfer analysis of the space shuttle orbiter wing subjected to reentry aerodynamic heating. By adding sufficient external forced convective cooling near the end of the heating cycle, the calculated surface temperatures of the thermal protection system (TPS) agree favorably with the flight data for the entire flight profile. However, the effects of this external forced convective cooling on the structural temperatures were found to be negligible. Both free convection and forced convection elements were introduced to model the internal convection effect of the cool air entering the shuttle interior. The introduction of the internal free convection effect decreased the calculated wing lower skin temperatures by 20°F at most, 1200 sec after touchdown. If the internal convection is treated as forced convection, the calculated wing lower skin temperatures after touchdown can be reduced to match the flight-measured data very closely. By reducing the TPS thicknesses to certain effective thicknesses to account for the TPS gap heating, the calculated wing lower skin temperatures prior to touchdown can be raised to agree with the flight data perfectly.

Introduction

Thermal behavior of the space shuttle orbiter structure subjected to the reentry aerodynamic heatings has been extensively analyzed by Ko, Quinn, Gong, Schuster, and Gonzales.¹⁻⁵ The authors used the newly developed structural performance and resizing (SPAR) finite-element thermal analysis computer program⁶ to calculate shuttle structural temperatures. The predicted and flight-measured structural temperatures agreed fairly well at most of the structure stations. However, in some structural locations (such as the wing lower skin and fuselage bottom skin), the structural temperature predictions were unsatisfactory for the time region after touchdown.

In the authors' earlier work,¹⁻⁵ the effect of the internal convection (free convection or forced convection) of the air mass inside the shuttle structure was neglected because the earlier (level 16 version) SPAR thermal analysis program could not handle the free convection. During the shuttle reentry flight, the outside cool air is allowed to enter the interior of the shuttle at 1400 sec from reentry (or at 100,000 ft altitude). This cool air mass could cool the shuttle structure to some degree. In addition, opening the vents at the shuttle wing roots prior to touchdown may cause the interior cool air to flow, creating some

forced convection. Neglecting the internal convection effect in previous thermal analysis could have caused the predicted structural temperatures in the aforementioned regions to be higher than the measured structural temperatures after touchdown, as shown in Fig. 1.

Another cause of the discrepancies between the predicted and the measured structural temperatures could be the insufficient negative heating (or forced convective cooling) near the end of the heat input cycle used in previous thermal analysis (see Fig. 2). More recent versions (level 25, Aug. 1983 and level 26, May 1984) of the SPAR thermal analysis program can handle the free convection effect. Therefore, the purpose of this report is to introduce both the free and forced convection elements to an existing SPAR thermal model for the shuttle wing, and to show how each type of internal convection affects the correlation between the predicted and the measured structural temperatures. Also discussed are the effects of TPS gap heatings and of the revised heat input with proper intensity of forced convective cooling (negative heating) near the end of the reentry flight.

Nomenclature

C41	four-node forced convection element
C53	five-node free convection element
C_i	characteristic lengths used in computing heat transfer coefficients, in
FC GEOM	SPAR computer program data set name for computing free convection heat transfer coefficients
h	TPS thickness, in
\bar{h}	effective TPS thickness, in
J_1 to J_4	fluid nodes for free convection
JLOC	joint location (or node, or grid point)
NI	SPAR index used in SPAR program
NJ	SPAR index used in SPAR program
SPAR	structural performance and resizing
STS-5	space transportation system, flight 5
THEOSKIN	theoretical skin heating
TPS	thermal protection system

*Aerospace Engineer, Aerostructures Branch.
Member AIAA.

**Aerospace Engineer, Aerostructures Branch.

T_{80}	wing lower skin temperature calculated using 80-percent TPS thickness, °F
T_{100}	wing lower skin temperature calculated using 100-percent TPS thickness, °F
T_{data}	flight-measured wing lower skin temperature, °F
t	time, sec
V_i	fluid volumes for free convection
V07T, V09T	thermocouple identification number
WS	wing segment
y_0	station in y axis

Subscripts:

i index, $i=1,2,3,4$

Description of Problem

The discussions in this report are limited to the thermal analysis of the wing segment WS240 shown in Fig. 3. The heat input to the thermal model is based on the actual trajectory (represented by circle, diamond, and triangle symbols) of space transportation system, flight 5 (STS-5) shown in Fig. 4. The WS240 thermal model, without the internal convection elements used in the previous thermal analysis,⁴ is shown in Fig. 5. The STS-5 surface heating rates previously input to the thermal model WS240 are presented in Fig. 2. Notice that most of the heating curves for the TPS surface stations have little cooling (negative heating because of forced convective cooling) near the ends of the heating cycles. The heating rates shown in Fig. 2 generated agreement between the calculated and the measured TPS surface temperatures for most of the reentry profile shown in Fig. 6. However, during a narrow time span near touchdown point, the measured lower TPS surface temperatures show more surface coolings. The WS240 substructural temperatures previously calculated using the STS-5 heat input are shown in Fig. 1. For the upper skin, the predicted and the flight-measured structural temperatures agreed reasonably well. However, the predicted and the measured structural temperatures for the lower skin agreed reasonably well up to touchdown. After that point the data and prediction compare poorly. The measured lower skin temperatures consistently show lower values. The purpose of this study was to improve the forced convective cooling near the end of the surface heating cycle, to introduce the internal free or forced convection elements to the existing WS240 thermal model (with or without the effect of TPS gap heatings), and finally to demonstrate how the inclusion of convection effects could improve structural temperature predictions.

Internal Convections

The exact nature of the airflow inside the shuttle wing after the introduction of the exter-

nal air and after the opening of vents at the wing root was unknown. Therefore, two types of internal convections were considered: (1) free convection and (2) forced convection.

Free Convection. — Fig. 7 shows the five-node free-convection elements C53 introduced inside the four bays of the WS240 thermal model. Because there are four surfaces of different orientations for each bay, four fluid nodes (located at the same joint location) had to be used for generating the C53 elements. For each bay, each fluid node is associated with each of the four smooth surfaces (no corners). Temperatures of the fluid nodes were not specified during the time period from the initiation of reentry ($t = 0$ sec) to 1400 sec. Afterwards the fluid nodal temperatures were set equal to the ambient air temperatures in order to simulate the entering of outside cool air into the shuttle structure at $t = 1400$ sec, or 100,000 ft altitude.

Figure 8 shows characteristic lengths C_i ($i=1,2,3,4$), and fluid volumes V_i ($i=1,2,3,4$) associated with each surface of a typical bay used in the construction of data set called FC GEOM (NASA CR-159162, SPAR Thermal Analysis Processors Reference Manual, revision (level) 26, May 1984) in the calculations of internal free convection heat transfer.

Forced Convection. — After opening the landing gear doors and vents at the wing roots, external air will enter the shuttle wing and induce convective heat transfer. In order to account for this effect, four-node forced convection elements C41 (replacing C53 elements) were introduced on the interior surfaces of four bays of the WS240 thermal model. The heat transfer coefficients for the C41 elements were calculated using the effective air flow velocities inside the four bays, listed in Table 1.

The effective air flow velocities of Table 1 were obtained from the aeroscience section of the shuttle prime contractor. The forced convective heat transfer coefficients were calculated using classic pipe flow theory.⁷ The natural convective heat transfer coefficient was computed by the equations given in Ref. 8 for free convection in enclosed plane gas layers. As will be shown, the heat transfer coefficients of Table 1 caused the calculated lower skin temperatures after touchdown to be in good to excellent agreement with the measured data.

External Forced Convection

The aerodynamic heating rates used in the SPAR thermal analyzer were computed by a NASA computer program called theoretical skin heating (THEOSKIN). The heat transfer coefficients calculated in this program were computed by the methods described in Refs. 4 and 9. The THEOSKIN program solves the one-dimensional thin-skin heating equation.¹⁰ For this equation, the thermal capacity is assumed to be constant. The TPS surface temperatures predicted by the THEOSKIN program are very close to the actual measured surface temperatures, and close to the SPAR-predicted surface temperatures for most of the flight pro-

file. However, during the latter part of the flight (approximately 1500 sec to end of rollout), this program calculated surface temperatures that were significantly lower than the measured values. These lower temperatures occurred primarily because heat was added to the TPS surface by conduction from the hotter inner layers of the TPS. Because of these lower temperatures, the THEOSKIN program predicted unrealistic aerodynamic forced convection heating or cooling rates, or both. This problem was circumvented in the thermal analysis of Refs. 1 to 5 by assuming the heating rates were zero beginning at 1500 sec to the end of rollout. To improve the accuracy of the calculated heating rates, the measured TPS surface temperatures were input to the THEOSKIN program for the flight profile times of 1500 to 1900 sec, and new heating rates were calculated (Fig. 9). These new heating rates (between 1500 and 1900 sec) were negative and, therefore, produced forced convective cooling for this portion of the flight profile.

TPS Gap Heating

In the previous thermal analysis of the space shuttle wing, both 80- and 100-percent TPS thicknesses were used for the wing lower surface.⁴ The 80-percent TPS thickness is an effective thickness used to approximate the effect of the TPS gap heating. The measured wing lower skin temperatures before touchdown always lie between the two curves of wing lower skin temperatures calculated by using 80- and 100-percent TPS thicknesses. The use of 80-percent TPS thickness resulted in overestimating the wing lower skin temperatures.⁴

Because the boundary layer thickness increases with the flow distance, the effect of TPS gap heating will decrease with the flow distance. Thus, the effective TPS thickness must vary with the flow distance. Effective TPS thickness for the wing lower surface may be calculated from the following empirical equation:

$$\bar{h} = h \left[1 - \frac{T_{\text{data}} - T_{100}}{T_{80} - T_{100}} (1 - 0.8) \right] \quad (1)$$

where

T_{80} = wing lower skin temperature at time t before touchdown, calculated by using 80-percent TPS thickness

T_{100} = wing lower skin temperature at time t before touchdown, calculated by using 100-percent TPS thickness

T_{data} = flight-measured wing lower skin temperature at time t before touchdown

h = 100-percent TPS thickness

\bar{h} = effective TPS thickness

Using this equation, the effective TPS thicknesses for the wing lower surface for WS240 (in STS-5) were:

Bay	\bar{h}/h
1	0.939
2	0.952
3	0.95
4	0.97

These \bar{h} values were used for the case in which internal forced convection was introduced.

Results

TPS Surface Temperatures

Figure 10 shows calculated and flight-measured TPS surface temperatures, based on the heating rates shown in Fig. 9. The correlation between the calculated and the measured data is quite good for the entire flight profile. Because sufficient forced convective cooling was introduced prior to touchdown (Fig. 9), the calculated TPS surface temperature curves exhibit a satisfactory valley before touchdown and follow the flight data closely.

Structural Temperatures

Figure 11 shows the comparison of calculated structural temperatures and the flight-measured temperatures. The structural temperatures shown by the dashed curves were calculated using 100-percent TPS thickness and using the revised external forced convective cooling. These structural temperatures are essentially the same as the structural temperatures calculated with little external forced convective cooling (Fig. 1). The structural temperatures with the introduction of internal free convection effect (using 100-percent TPS thickness) are shown by solid curves, and structural temperatures with the introduction of the internal forced convection effect (using effective TPS thickness) is shown by long-short dashed curves. The correlation between the calculated and the measured structural temperatures is satisfactory for the upper skin for the entire flight profile. The correlation was very good for the lower skin up to touchdown, if the effective TPS thickness is used. The effect of internal free convection decreased the wing lower skin temperatures by a maximum of 20°F at 1200 sec after touchdown, but did not cause the lower skin temperature curves to drop low enough to follow the flight data after touchdown. For the case with the effect of forced internal convection, the calculated wing lower skin temperature curves follow the measured data almost perfectly after touchdown for bays 1, 2, and 3 and fairly good for bay 4. This indicates that the internal convection prior to touchdown is forced convection. The slight difference between the data and the forced convection curve for bay 4 after touchdown may be attributed to the thermal interaction with the elevon structure, which was neglected in the SPAR thermal analysis.

Conclusions

Finite-element heat transfer analysis was performed on the shuttle wing segment subjected to

STS-5 reentry heating. With the introduction of sufficient external forced convective cooling near the end of the heating cycle, the calculated TPS surface temperatures followed the flight data for the entire flight profile; the correlation between the calculated and measured TPS surface temperatures became nearly perfect during the cooling time region immediately prior to touchdown. However, this improved agreement had negligible effects on the structural temperatures.

Internal free convection lowered the calculated wing lower skin temperatures by a maximum 20°F at 1200 sec after touchdown, but did not cause calculated wing lower skin temperatures to decrease enough to fit the flight data after touchdown.

By treating the internal convection as forced convection, the calculated wing lower skin temperatures after touchdown could be lowered enough to fit the flight data almost perfectly for bays 1, 2, and 3 and fairly good for bay 4.

Using the effective TPS thickness for the wing lower surface to account for the TPS gap heating, the calculated and measured wing lower skin temperatures prior to touchdown agreed very well.

References

¹Ko, William L., Quinn, Robert D., Gong, Leslie, Schuster, Lawrence S., and Gonzales, David, "Preflight Reentry Heat Transfer Analysis of Space Shuttle," AIAA 81-2382, Nov. 1981.

²Ko, William L., Quinn, Robert D., Gong, Leslie, Schuster, Lawrence S., and Gonzales, David, "Reentry Heat Transfer Analysis of the Space

Shuttle Orbiter," Computational Aspects of Heat Transfer in Structures. NASA CP-2216, 1982, pp. 295-325.

³Gong, Leslie, Quinn, Robert D., and Ko, William L., "Reentry Heating Analysis of Space Shuttle with Comparison of Flight Data," Computational Aspects of Heat Transfer in Structures. NASA CP-2216, 1981, pp. 271-294.

⁴Gong, Leslie, Ko, William L., and Quinn, Robert D., "Thermal Response of Space Shuttle Wing During Reentry Heating," NASA TM-85907, 1984.

⁵Ko, William L., Quinn, Robert D., and Gong, Leslie, "Finite Element Reentry Heat Transfer Analysis of Space Shuttle Orbiter," NASA TP-2657, 1986.

⁶Marlowe, M.B., Moore, R.A., and Whetstone, W.D., "SPAR Thermal Analysis Processors Reference Manual, System Level 16," NASA CR-159162, 1979.

⁷Schlichting, H., Boundary-Layer Theory, 4th ed., McGraw-Hill Book Co., 1960.

⁸Jakob, Max, Heat Transfer, 5th ed., Vol. 1, John Wiley and Sons, Inc., 1956.

⁹Zoby, E.V., Moss, J.N., and Sutton, K., "Approximate Convective-Heating Equations for Hypersonic Flows," J. Spacecraft and Rockets, Vol. 18, Jan. 1981, pp. 64-70.

¹⁰Quinn, Robert D. and Palitz, Murray, "Comparison of Measured and Calculated Turbulent Heat Transfer on the X-15 Airplane at Angles of Attack up to 19.0°," NASA TMX-1291, 1966.

Table 1. — Effective air flow velocities and associated heat transfer coefficients for internal forced convection (bays 1 to 4)

Time, sec	Effective air flow velocity, ft/sec	Heat transfer coefficient, Btu/sec-in ² -°F
1750	25	3.30×10^{-6}
1850	25	4.00×10^{-6}
2000	15	2.73×10^{-6}
3000	0	0.35×10^{-6} *

* 0.35×10^{-6} is the heat transfer coefficient for natural convection.

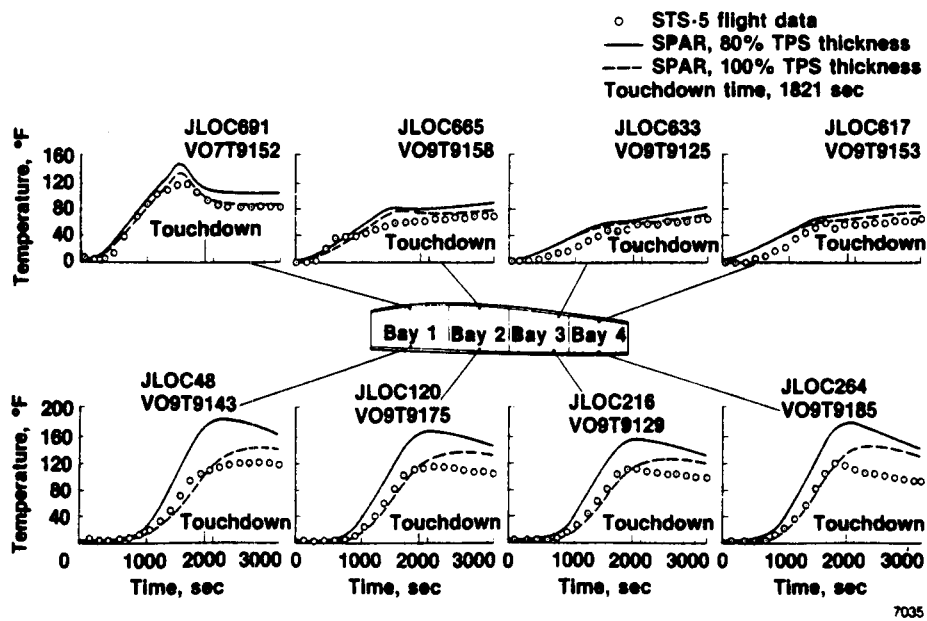


Figure 1. Time histories of structural temperatures for WS240 without internal convection, STS-5 flight (ref. 4, fig. 15).

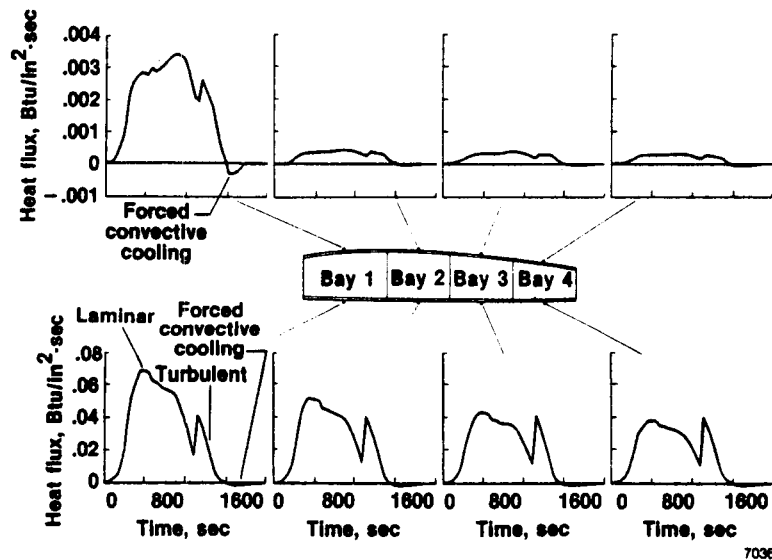
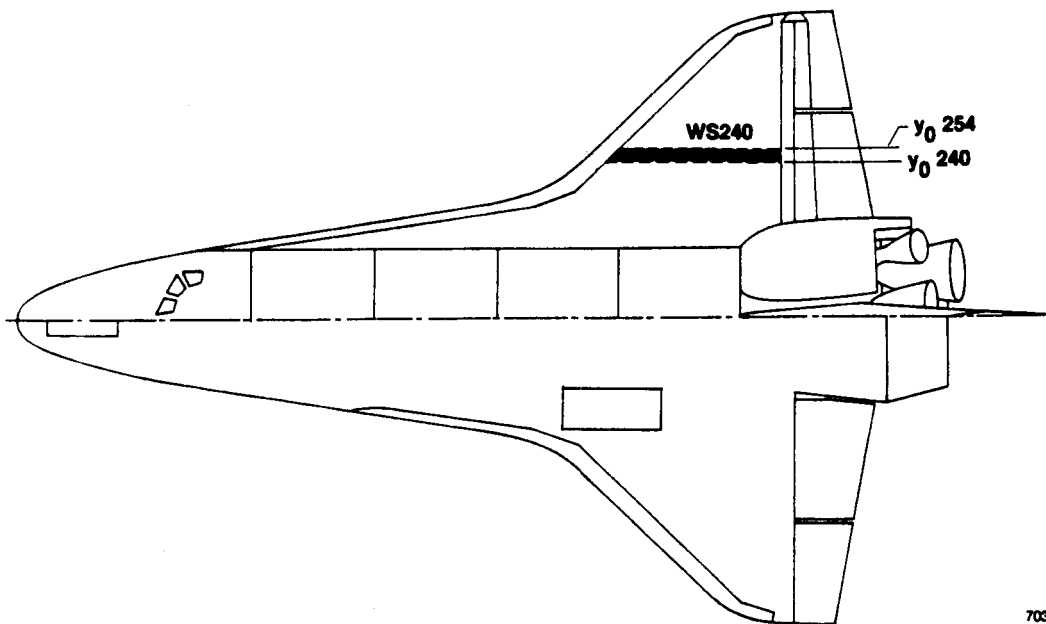
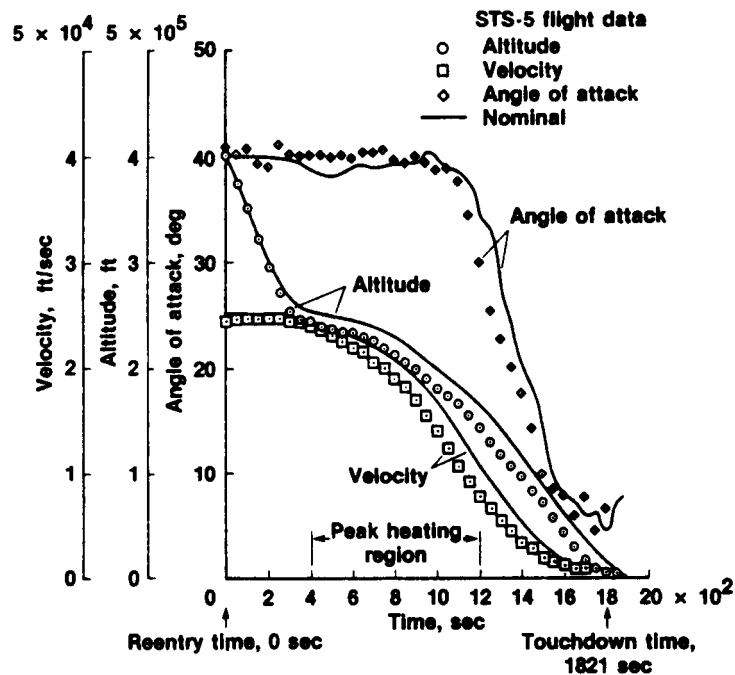


Figure 2. Surface heating rates at WS240 without sufficient external forced convective cooling STS-5 (ref. 4, fig. 9).



7037

Figure 3. Locations of space shuttle wing segment that were analyzed.



7038

Figure 4. STS-5 reentry trajectory.

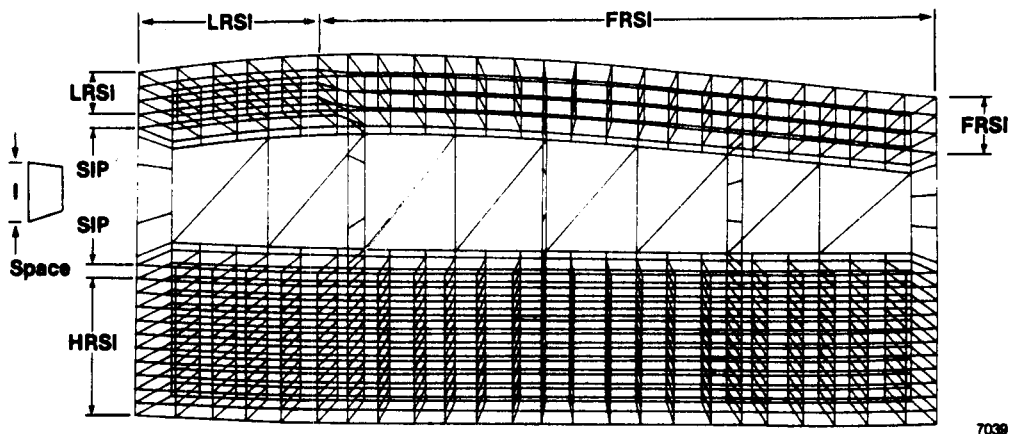


Figure 5. Three-dimensional SPAR finite-element thermal model for WS240 and 920 JLOC. No free convection elements.

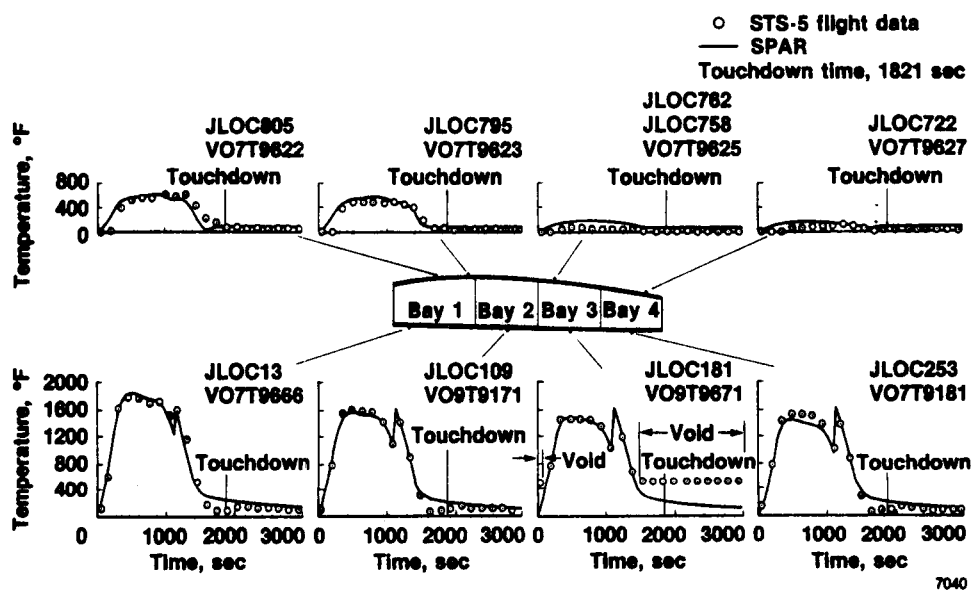


Figure 6. Time histories of TPS surface temperatures for WS240, STS-5 flight (ref. 4, fig. 14).

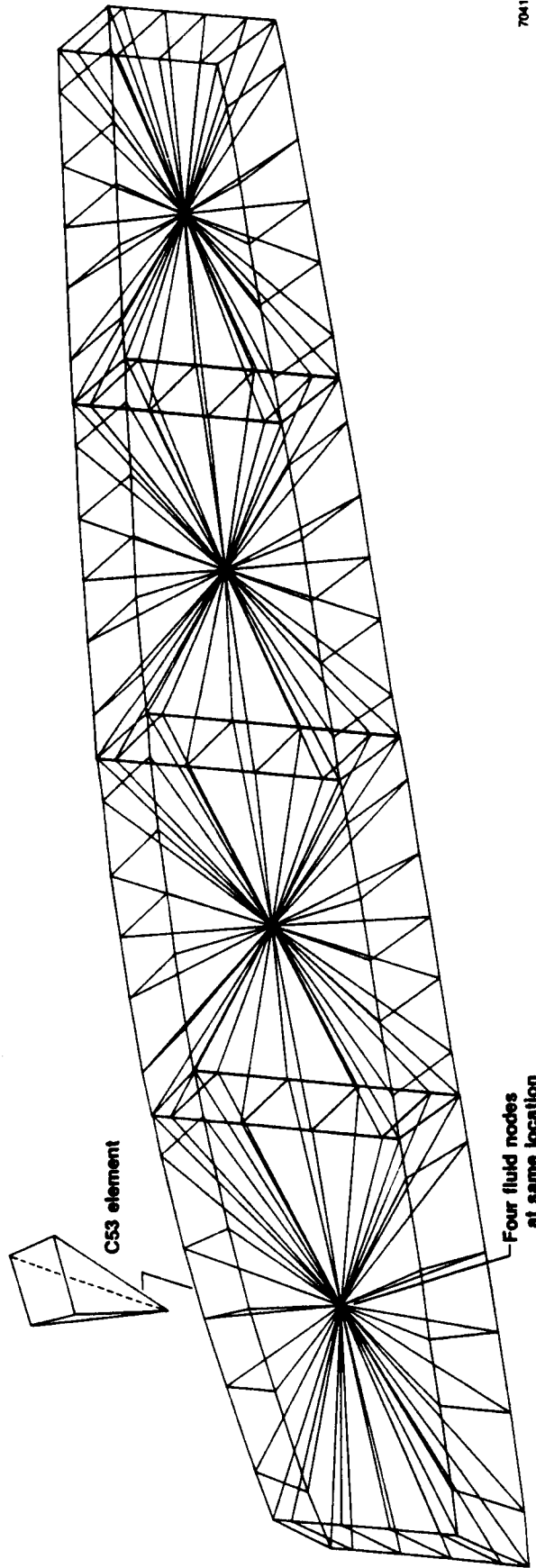


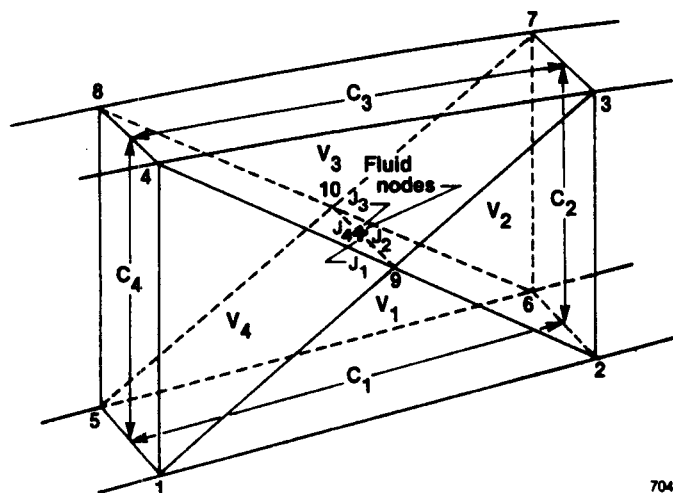
Figure 7. Five-node free convection elements C53 set up inside the four bays of WS240.

7041

$V_1 = 1, 2, 9, 5, 6, 10$
 $V_2 = 2, 3, 8, 6, 7, 10$
 $V_3 = 3, 4, 9, 7, 8, 10$
 $V_4 = 4, 1, 9, 8, 5, 10$

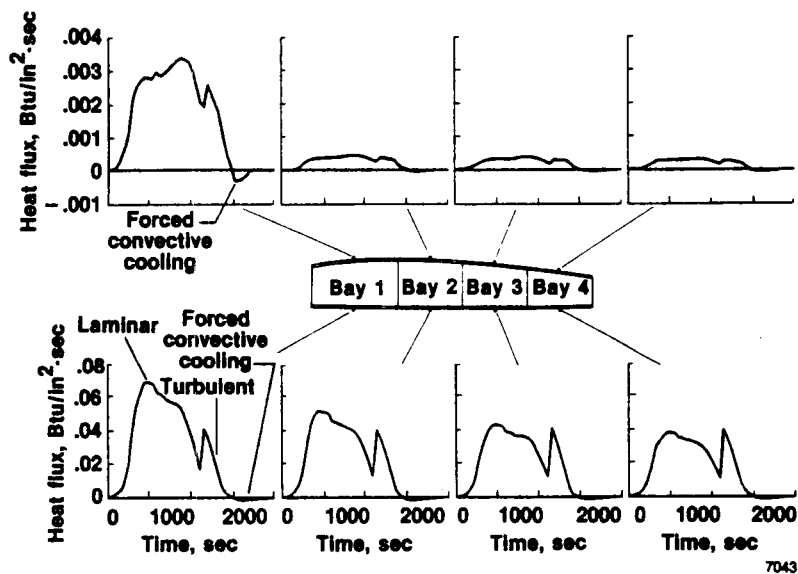
Table (NI = 3, NJ = 4); FC GEOM 1 1
 I = 1,3; J = 1,4

J_1	C_1	V_1
J_2	C_2	V_2
J_3	C_3	V_3
J_4	C_4	V_4



7042

Figure 8. Fluid nodes, characteristic lengths C_i and fluid volumes V_i for a typical bay for constructing data set "FC GEOM."



7043

Figure 9. Surface heating rates at WS240 with sufficient external forced convective cooling, STS-5 flight.

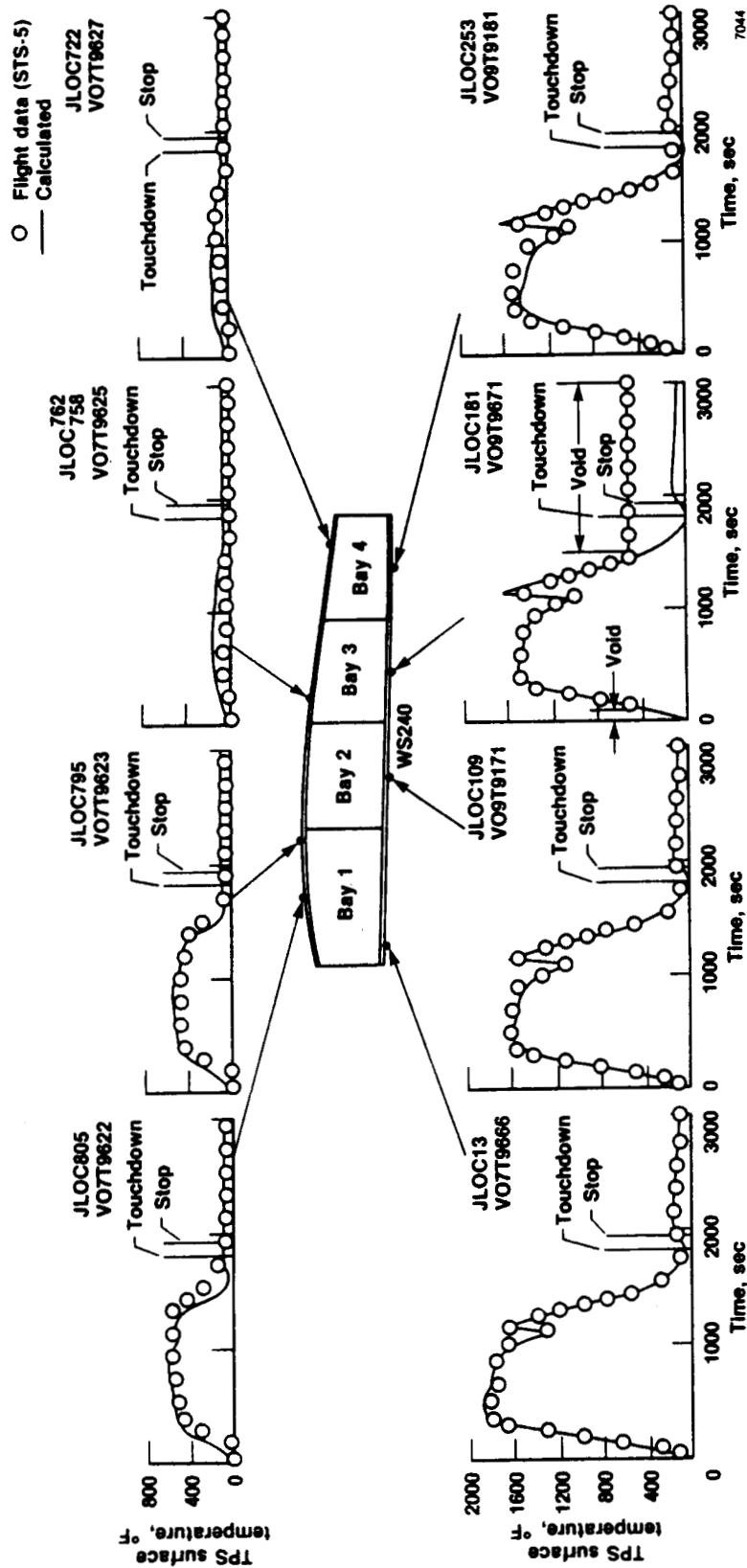


Figure 10. Time histories of TPS surface temperatures for WS240, STS-5 flight.

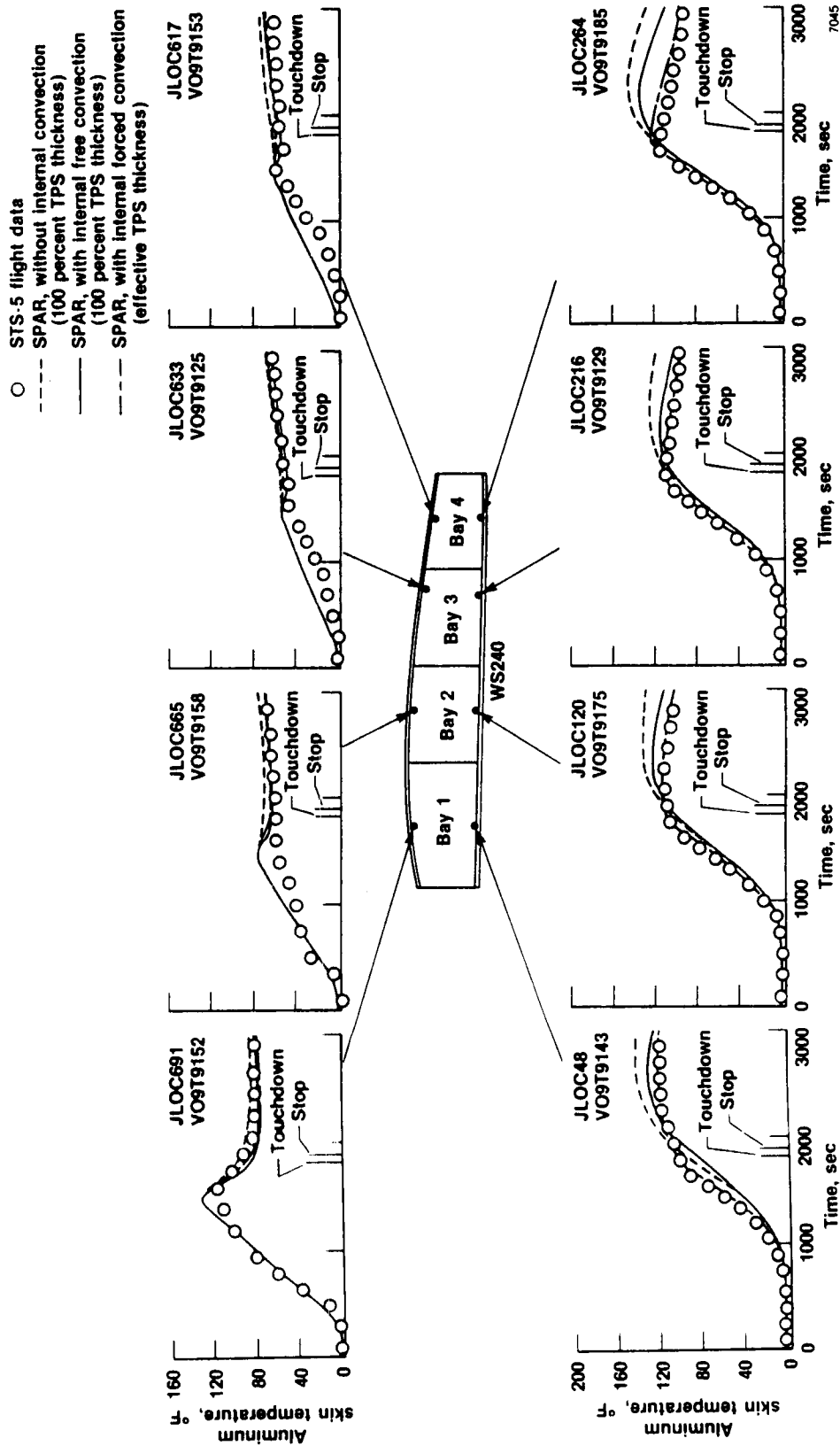


Figure 11. Time histories of structural temperatures for WS240 with internal convection, STS-5 flight.

1. Report No. NASA TM-86800 Revision		2. Government Accession No.		3. Recipient's Catalog No.	
4. Title and Subtitle Effects of Forced and Free Convections on Structural Temperatures of Space Shuttle Orbiter During Reentry Flight				5. Report Date October 1986 Revised June 1987	
				6. Performing Organization Code	
7. Author(s) William L. Ko, Robert D. Quinn, and Leslie Gong				8. Performing Organization Report No. H-1414	
9. Performing Organization Name and Address NASA Ames Research Center Dryden Flight Research Facility P.O. Box 273 Edwards, CA 93523-5000				10. Work Unit No. RTOP 505-53-51	
				11. Contract or Grant No.	
12. Sponsoring Agency Name and Address National Aeronautics and Space Administration Washington, D.C. 20546				13. Type of Report and Period Covered Technical Memorandum	
				14. Sponsoring Agency Code	
15. Supplementary Notes Prepared as AIAA-87-1600 for presentation at the AIAA 22nd Thermophysics Conference, Honolulu, Hawaii, June 8-10, 1987.					
16. Abstract <p>Structural performance and resizing (SPAR) finite-element thermal analysis computer program was used in the heat transfer analysis of the space shuttle orbiter wing subjected to reentry aerodynamic heating. With sufficient external forced convective cooling near the end of the heating cycle, the calculated surface temperatures of the thermal protection system (TPS) agree favorably with the flight data for the entire flight profile. However, the effects of this external forced convective cooling on the structural temperatures were found to be negligible. Both free convection and forced convection elements were introduced to model the internal convection effect of the cool air entering the shuttle interior. The introduction of the internal free convection effect decreased the calculated wing lower skin temperatures by 20°F at most, 1200 sec after touchdown. If the internal convection is treated as forced convection, the calculated wing lower skin temperatures after touchdown can be reduced to match the flight-measured data very closely. By reducing the TPS thicknesses to certain effective thicknesses to account for the TPS gap heating, the calculated wing lower skin temperatures prior to touchdown can be raised to agree with the flight data perfectly.</p>					
17. Key Words (Suggested by Author(s)) Forced convection Space shuttle wing Heat transfer STS-5 data Natural convection Structural temperatures Reentry heating TPS temperatures				18. Distribution Statement Unclassified — Unlimited Subject Category 34	
19. Security Classif. (of this report) Unclassified		20. Security Classif. (of this page) Unclassified		21. No. of Pages 13	
				22. Price* A02	

**For sale by the National Technical Information Service, Springfield, Virginia 22161.*